TECHNICAL NOTE

Fourier-Transform Infrared Spectroscopy Analysis of the Changes in Chemical Composition of Wooden Components: Part II—The Ancient Building of Danxia Temple

Yan Yang He Sun Shuang Yang Wenye Sun Ying Zhao
Bin Li Wei Wang Xiaoqian Zhang Shilong Jiang Qian Xu

Abstract

To investigate the decay extent of wooden components in the ancient buildings of Danxia Temple, the absorption peak intensities, changes in chemical components, and cellulose crystallinity of red oak (*Quercus* sp.), birch (*Betula* sp.), and maple (*Pterocarya* sp.) wooden components were determined and analyzed using Fourier-transform infrared spectroscopy. The results are as follows: (1) The absorption peak intensities representing cellulose and hemicellulose decreased or disappeared obviously in the decayed red oak wood (DROW); on the contrary, those representing lignin increased. The indexes of the content of cellulose, hemicellulose, and cellulose crystallinity also decreased; on the contrary, those of the content of lignin increased. Those results indicated that cellulose and hemicellulose in DROW were largely degraded by brown-rot fungi. (2) The absorption peak intensities representing cellulose and hemicellulose decreased both in the decayed birch wood (DBW) and the decayed maple wood (DMW), whereas those representing lignin increased. The indexes of the content of cellulose, hemicellulose, and cellulose crystallinity also decreased, whereas those of lignin increased. Those results showed that cellulose and hemicellulose in DBW and DMW were seriously harmed not only by insects but also by brown-rot fungi. By comparison, the extent of fungal damage was lower in DMW than in DBW.

The Danxia Temple, with wooden structures, was first built in about 824 A.D. and is located in Liushan Town, Nanzhao County, Nanyang City, Henan Province, China. It is a national cultural relics protection unit and is one of the eight famous temples in Henan Province. It is of great historical, scientific (as an example of historical material civilization), and artistic value. However, under the influence of factors such as ambient temperature, humidity, microorganisms, insects, light, and so on, some wooden components, especially the roots of wooden pillars, have been degraded to different degrees.

It is well known that degradation inevitably leads to the change of anatomical structures (Murace et al. 2006; Win et al. 2008; Padhiar and Albert 2011, 2012; Sanghvi et al. 2013; Koyani and Rajput 2014; Bhatt et al. 2016; Bari et al. 2019, 2020; Diandari et al. 2020; Yang et al. 2020a), chemical components (Ferraz and Durán 1995; Arias et al. 2010; Bari et al. 2019, 2020; Girometta et al. 2020; Sun et al. 2020; Yang et al. 2020b), and reduction in physical and mechanical properties (Choi et al. 2006; Brischke et al. 2019; Chang et al. 2019; Gao et al. 2019; Li et al. 2019; Bari et al. 2020). These reductions eventually affect the safety and the life span of the ancient buildings. The three main chemical components of wood, i.e., cellulose, hemicellu-

The authors are, respectively, Associate Professor, School of Architecture, Nanyang Inst. of Technol., Nanyang City, Henan Province, China (yangyanrainy@163.com [corresponding author]); Doctoral Candidate, College of Materials Sci. and Engineering, Southwest Forestry Univ., Kunming City, Yunnan Province, China (1066659587@qq.com); Undergraduate, School of Economics, Henan Univ. Minsheng College, Kaifeng City, Henan Province, China (2729153423@qq.com); Undergraduate, Undergraduate, Associate Professor, Lecturer, Undergraduate, Undergraduate, and Undergraduate, School of Architecture, Nanyang Inst. of Technol., Nanyang City, Henan Province, China (1932741108@qq.com, 2624451772@qq.com, 165400683@qq.com, 659774129@qq.com, 1317962674@qq.com, 2213762790@qq.com, 1954416628@qq.com). This paper was received for publication in March 2021. Article no. 21-00015.

Forest Prod. J. 71(3):283–289.
doi:10.13073/FPJ-D-21-00015

lose, and lignin, have corresponding characteristic infrared absorption spectra. The absorption peaks of 1,735 cm^{-1}, 1,374 cm^{-1}, and 897 cm^{-1} correspond to functional group C=O stretching that represents hemicellulose, C-H stretching that represents holocellulose, and C-H stretching that represents cellulose, respectively in Fourier-transform infrared (FTIR) spectroscopy characteristic spectra (Table 1). Those of 1,600 cm^{-1} and 1,508 cm^{-1}, 1,460 cm^{-1}, 1,424 cm^{-1}, and 1,260 cm^{-} correspond to the aromatic skeleton stretching, C-H deforming, CH_2 bending, and C-O stretching, respectively, which represent lignin (Table 1) (Pandey and Pitman 2003; Stark and Matuana 2004, 2007; Ibrahim et al. 2007; Pandey and Nagveni 2009, Li et al. 2010; Monrroy et al. 2011; Zeng et al. 2012; Tomak et al. 2013; Xu et al. 2013; Liu et al. 2017; Tamburini et al. 2017; Croitoru et al. 2018; Fahey et al. 2019; Wentzel et al. 2019; Bari et al. 2020; Dong et al. 2020; Sun et al. 2020). The shapes, positions, and intensities of the absorption peaks in FTIR spectra will change, as will the chemical components of woods. Therefore, the changes of wood functional groups and the contents of the three main chemical components can be determined according to the changes (increase, decrease, or disappearance) of the absorption peak intensities in the FTIR characteristic spectra.

The FTIR spectroscopy method is helpful to evaluate the changes of chemical components of woods. The method has some advantages, such as only requiring a minimal number of samples (about a few milligrams) (Pandey and Pitman 2003, Xu et al. 2013, Yang et al. 2020b) and results in less damage to ancient buildings (Yang et al. 2020 b) compared with conventional gravimetric techniques. It is increasingly used to study the deterioration extent and evaluate current bearing capacity of wooden components in ancient buildings.

The goals of this study were to determine the changes in chemical components and investigate the degradation extent and mechanism of wood components with FTIR analysis in the ancient buildings of Danxia Temple. The results of this study provide reliable data support and guidance for later protection and repair of wooden components of cultural relics.

Materials and Methods

Materials

Three samples were collected from wooden components in the ancient buildings of Danxia Temple in Nanzhao County, Nanyang City, Henan Province, China. The first sample, identified as red oak wood (*Quercus* sp.), was obtained from the root of the wooden pillar in the Tianwang Hall. The second sample, identified as birch wood (*Betula* sp.), was obtained from the root of the wooden pillar in the Pilu Hall. The third sample, identified as maple wood (*Pterocarya* sp.), was obtained from the root of the wooden pillar in the Tianran Ancestor's Hall. The samples were taken with an increment borer (10-100-1027, Haglöf AB, Mora, Sweden,). The first sample was degraded seriously by fungi, whereas the second and third samples showed signs of insect attack visible to the naked eye (Fig. 1). Control samples were obtained at the location of 1 m from the living tree roots about 10 years old and 30-cm breast diameter by increment borer (10-100-1027, Haglöf) and they were dried before FTIR testing. The wood powder needed for FTIR analysis was processed using an agate mortar.

FTIR testing

For FTIR analysis, oven-dried wood powder and spectrum KBr were fully mixed in a ratio of 1:150, poured into an agate mortar, and ground into powdered form while keeping the wood powder and KBr in dried condition by using a high-wattage lamp throughout the whole process. The powder mixture (about a few milligrams) was compressed into sliced samples using a powder tablet press machine (FW-5A, Uncommon Technology Development Co., China).

Table 1. Fourier-transform infrared spectroscopy characteristic bands of the wood samples studied.

Wave number (cm^{-1})	Functional groups	Main band assignments and explanations
1,735	C=O	C= O stretching in unconjugated ketone, carbonyl, and aliphatic groups (hemicelluloses)
1,649	C=O	C= O stretching in conjugated carbonyl groups (lignin)
1,600	C=C, C=O	Aromatic skeleton stretching, C= O stretching, stronger syringyl unit than guaiacyl unit
1,508	C=C	Aromatic skeleton stretching, stronger guaiacyl unit than syringyl unit
1,460	C-H	C-H deforming in methyl (asymmetry in -CH and -CH2) (lignin), CH_2 deformation stretching (lignin and polyxylose)
1,424	C-H	CH_2 shear vibration (cellulose); aromatic skeleton bending (lignin)
1,374	C-H	C-H stretching (cellulose and hemicellulose)
1,336	C-O, C-H	Condensation of guaiacyl unit and syringyl unit (lignin), syringyl unit and CH_2 bending (cellulose)
1,316–1,320	C-H	CH_2 shear vibration, O-H in-plane bending (cellulose and hemicellulose)
1,260	C-O	C-O stretching of mainly guaiacyl unit (lignin)
1,245	C-O-C	C-O-C stretching in phenol–ether bonds of lignin (lignin)
1,232	C-C, C–O	C-C, C-O stretching (lignin)
1,200	C–O–C	C–O–C symmetrical bending, O-H in-plane bending (cellulose and hemicellulose)
1,159	C-O-C	C-O-C stretching (cellulose and hemicellulose)
1,137	C-H	C-H in-plane bending in guaiacyl units (lignin)
1,120	C-H	C-H in-plane bending in syringyl units (lignin)
1,112		Syringyl unit aromatic rings (lignin)
1,104	O-H	OH-associated absorption band (cellulose)
1,058	C-O	C-O deforming in secondary alcohols and aliphatic ethers (cellulose and hemicellulose)
1,039	C=O	C=O stretching (cellulose, hemicellulose, and lignin)
897	C-H	C-H bending (cellulose)
810		Mannose structure (hemicellulose)

(a) (b) (c)

Figure 1.—Locations of sampling in Danxia Temple. (a) Sample no. 1. (b) Sample no. 2. (c) Sample no. 3.

FTIR spectra were generated using a FTIR spectrophotometer (ALPHA2, Bruker Inc., Germany) in the range of 4,000 to 400 cm^{-1} to provide detailed information on the functional groups present in the sample surface (Yang et al. 2015, 2020c). Scans were run at a resolution of 4 cm^{-1} and the spectra were obtained using attenuated total reflectance. To avoid the effect of experimental error, a minimum of five scans per specimen was run to calculate their average.

Analysis of the changes in chemical components

To eliminate the differences of wood powder content and the influence of operation error on the experimental results in the experimental process, the stable absorption peak of 1,508 cm^{-1} representing aromatic skeleton stretching was taken as the standard, and the ratio of the absorption peak heights of cellulose or hemicellulose to lignin (1,508 cm^{-1}) was used to characterize the contents of chemical components (Pandey and Pitman 2003, Li et al. 2010, Xu et al. 2013, Liu et al. 2017).

The absorption peak height was calculated as follows: the tangent of the lowest point on both sides of the absorption peaks was taken as the baseline, and the vertical line was drawn from the end of the absorption peak to the baseline. The distance from the intersection of the vertical line and the baseline to the top of the absorption peak was the absorption peak height (Pandey and Pitman 2003, Li et al. 2010, Xu et al. 2013, Bari et al. 2020; Dong et al. 2020).

The content of lignin was characterized by the values of I1508/I1735 and I1508/I1374, whereas that of hemicellulose was characterized by I1735/I1508, that of cellulose by I897/I1508, and that of holocellulose by I1374/I1508 and I1159/I1508 (Li et al. 2010, Xu et al. 2013, Liu et al. 2017, Bari et al. 2020, Sun et al. 2020). The percentage of change in the amount of chemical component is calculated using Equation 1, whereas the retained amount is from Equation 2. In the calculation results, ''+'' indicates increase and ''–'' indicates decrease (Dong et al. 2020).

$$\text{Change amount of chemical component} = \frac{\text{peak height ratio in decayed wood} - \text{peak height ratio in nondecayed wood}}{\text{peak height ratio in nondecayed wood}} \times 100 \quad (1)$$

$$\text{Retained amount of chemical component} = \frac{\text{peak height ratio in decayed wood}}{\text{peak height ratio in nondecayed wood}} \times 100 \quad (2)$$

Analysis of change in cellulose crystallinity

The index of cellulose crystallinity in wood was characterized by the values of I1374/I2900 and I1429/I897 (Monrroy et al. 2011, Tomak et al. 2013, Yang et al. 2020b). The change amount and the retained amount of cellulose crystallinity is referred to Equations 1 and 2.

Results

FTIR analysis of the red oak wooden components

As can be seen from Figure 2, the absorption peak positions of decayed red oak wood (DROW) in the region from 1,800 to 800 cm^{-1} had no displacement, but the intensities had obvious changes. Compared with non-decayed red oak wood (NDROW), the absorption peak intensities of 1,735 cm^{-1}, 1,374 cm^{-1}, and 897 cm^{-1} were obviously decreased (Fig. 2), showing that cellulose and hemicellulose were largely degraded by decay fungi. In addition, the absorption peak intensities of 1,159cm^{-1} and 1,058cm^{-1}, which represent holocellulose, disappeared (Fig. 2), indicating that the degradation of holocellulose was more evident at these two absorption peaks. The decreases and disappearances of the absorption peak intensities eventually resulted in the decrease of the contents of cellulose and hemicellulose.

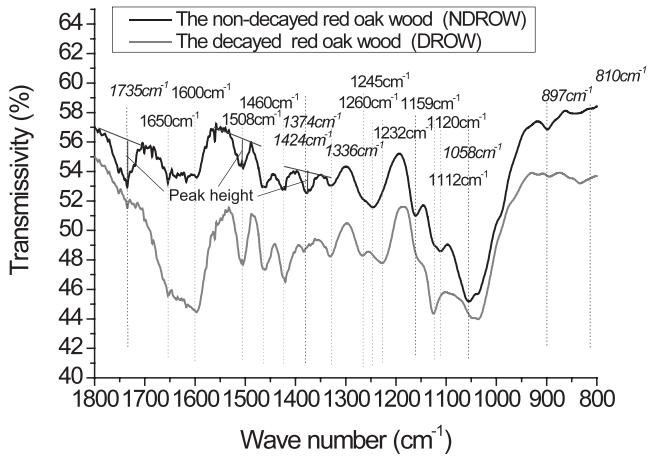

Figure 2.—Infrared spectrum of the red oak wooden component: region from 1,800 to 800 cm^{-1}.

Compared with NDROW, the absorption peak intensities of 1,600 cm^{-1}, 1,508 cm^{-1}, 1,460 cm^{-1}, 1,424 cm^{-1}, and 1,336 cm^{-1}, which represent lignin, increased, especially at 1,508 cm^{-1}, 1,424 cm^{-1}, and 1,460 cm^{-1} (Fig. 2), suggesting that the content of lignin increases in DROW. The absorption peak intensity of 1,245 cm^{-1}, which represents lignin, disappeared, but two new peaks were added at 1,260 cm^{-1} and 1,232 cm^{-1} (Fig. 2). Although the absorption peak of 1,112 cm^{-1} disappeared, a new absorption peak was added at 1,120 cm^{-1} (Fig. 2). The increases of lignin absorption peak intensities and the formations of the new peaks indicated that the lignin contents in DROW increased. In general, the increases in lignin contents also indicated a great increase in cellulose decomposition (Pandey and Pitman 2003, Pandey and Nagveni 2009).

As a rule, brown-rot fungi can attack both cellulose and hemicellulose and retain lignin; whereas white-rot fungi can consume cellulose, hemicellulose, and lignin, especially lignin (Guo et al. 2010); the selective removal of cellulose and hemicellulose suggests that the oak wood was decayed by brown-rot fungi.

Table 2 shows that the content of lignin in DROW increased by about 10-fold in I1508/I1735 and threefold in I1508/I1374, respectively, whereas those of cellulose and hemicellulose decreased. These findings agree with those previous studies (Yang et al. 2020a, Sun et al. 2020) and are also consistent with the visual spectrogram (Fig. 1). The index value of the cellulose crystallinity in I1374/I2900 decreased by 45.00 percent and that in I1424/I897 decreased by 21.05 percent (Table 2), indicating that the crystalline zones of cellulose were greatly degraded by brown-rot fungi (Monrroy et al. 2011). The reduction of the cellulose crystallinity naturally would also result in a reduction in physical and mechanical properties of wood components.

FTIR analysis of the birch wooden components

Compared with nondecayed birch wood, the absorption peak intensities at 1,735 cm^{-1}, 1,374 cm^{-1}, and 1,158 cm^{-1} in decayed birch wood (DBW) were clearly reduced (Fig. 3), indicating that both cellulose and hemicellulose were seriously degraded by rot fungi, resulting in a decrease of the contents of cellulose and hemicellulose; whereas those at 1,651 cm^{-1}, 1,598 cm^{-1}, 1,508 cm^{-1}, 1,460 cm^{-1}, 1,424 cm^{-1}, 1,336 cm^{-1}, 1,245 cm^{-1}, and 1,120 cm^{-1} in DBW increased significantly, especially at 1,508 cm^{-1}, 1,460 cm^{-1}, 1,424 cm^{-1}, and 1,336 cm^{-1} (Fig. 3), indicating an increase of lignin content in DBW. According to the results of Guo et al. (2010), DBW might be severely damaged by brown-rot fungi.

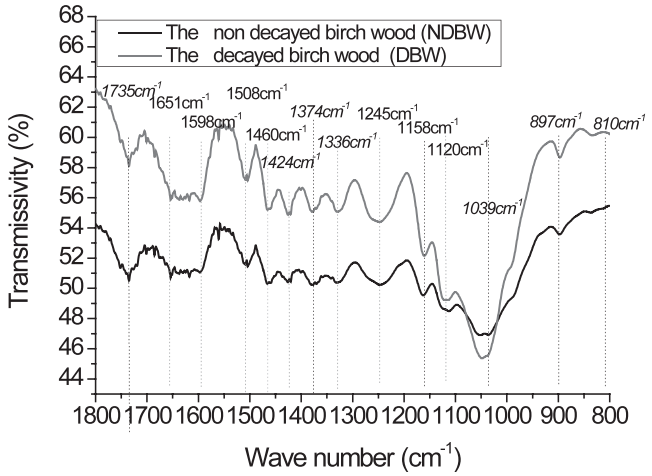

Figure 3.—Infrared spectrum of the birch wooden component: region from 1,800 to 800 cm^{-1}.

Table 2. Ratio of Fourier-transform infrared spectroscopy characteristic peak height of wood samples.

Samples	Absorption peak height ratio of lignin to cellulose or hemicellulose		Absorption peak height ratio of cellulose or hemicellulose to lignin				Index values of cellulose crystallinity	
	I1508/I1735	I1508/I1374	I1735/I1508	I1374/I1508	I1159/I1508	I897/I1508	I1374/I2900	I1424/I897
Red oak								
NDROW[a]	0.59	1.19	1.68	0.84	0.95	0.32	2.00	3.17
DROW	6.50	4.73	0.15	0.21	0.00	0.04	1.10	2.50
Difference	+5.91	+3.54	−1.53	−0.63	−0.95	−0.28	−0.90	−0.67
Remaining amount (%)	1094.74	398.09	9.13	25.12	0.00	12.18	55.00	78.95
Change amount (%)	+994.74	+298.09	−90.87	−74.88	−100.00	−87.82	−45.00	−21.05
Birch								
NDBW	0.65	1.88	1.53	0.53	0.60	0.33	0.80	1.54
DBW	1.09	3.00	0.92	0.33	0.42	0.33	0.33	1.01
Difference	+0.44	+1.13	−0.62	−0.20	−0.18	0.00	−0.47	−0.53
Remaining amount (%)	167.27	160.00	59.78	62.50	69.44	100.00	41.67	65.58
Change amount (%)	+67.27	+60.00	−40.22	−37.50	−30.56	0.00	−58.33	−34.42
Maple								
NDMW	0.67	0.47	1.50	2.13	2.19	0.25	2.43	3.00
DMW	5.83	7.00	0.17	0.14	0.00	0.11	0.36	1.57
Difference	+5.17	+6.53	−1.33	−1.98	−2.19	−0.14	−2.07	−1.43
Remaining amount (%)	875.00	1487.50	11.43	6.72	0.00	45.71	14.71	52.33
Change amount (%)	+775.00	+1387.50	−88.57	−93.28	−100.00	−54.29	−85.29	−47.67

[a] NDROW = nondecayed red oak wood; DROW = decayed red oak wood; NDBW = nondecayed birch wood; DBW = decayed birch wood; NDMW = nondecayed maple wood; DMW = decayed maple wood.

The content of lignin in DBW increased by 67.27 percent in I1508/I1735 and 60.00 percent in I1508/I1374, respectively, whereas those of cellulose and hemicellulose decreased evidently by 40.22 percent in I1735/I1508, 37.50 percent in I1374/I1508, and 30.56 percent in I1159/I1508, respectively, as shown in Table 2. The results further showed that cellulose and hemicellulose were seriously degraded and harmed not only by insects but also by brown-rot fungi. The results are consistent with the visual spectrogram (Fig. 3). The index value of the cellulose crystallinity in I1374/I2900 decreased by 58.33 percent and that in I1424/I897 decreased by 34.42 percent in DBW (Table 2), indicating that the crystalline zones of cellulose were also greatly degraded by brown-rot fungi (Monrroy et al. 2011).

FTIR analysis of the maple wooden components

Compared with nondecayed maple wood, the absorption peak intensities at 1,735 cm^{-1} and 1,374 cm^{-1} in decayed maple wood (DMW) was distinctly reduced (Fig. 4), indicating that cellulose and hemicellulose were degraded seriously by rot fungi. In addition, the absorption peaks at 1,158 cm^{-1} and 897 cm^{-1} in DMW disappeared (Fig. 4), indicating that the degradation of cellulose and hemicellulose was more obvious at these two absorption peaks. The decreases and disappearances of the absorption peak intensities resulted in a decrease of the contents of cellulose and hemicellulose.

Moreover, the absorption peak intensities at 1,650 cm^{-1}, 1,598 cm^{-1}, 1,508 cm^{-1}, 1,460 cm^{-1}, 1,424 cm^{-1}, 1,336 cm^{-1}, and 1,120 cm^{-1} in DMW increased significantly, especially at 1,508 cm^{-1}, 1,460 cm^{-1}, 1,424 cm^{-1}, 1,336 cm^{-1}, and 1,120 cm^{-1} (Fig. 4). The absorption peak at 1,245 cm^{-1} in DMW disappeared, but two new peaks were added at 1,260 cm^{-1} and 1,232 cm^{-1} (Fig. 4). The increases of absorption peak intensities and the formation of new peaks indicated the increase of lignin contents in DMW. According to the result (Guo et al. 2010) that brown-rot fungi can consume both celluloses and retain lignin, it was speculated that DMW was severely damaged by brown-rot fungi.

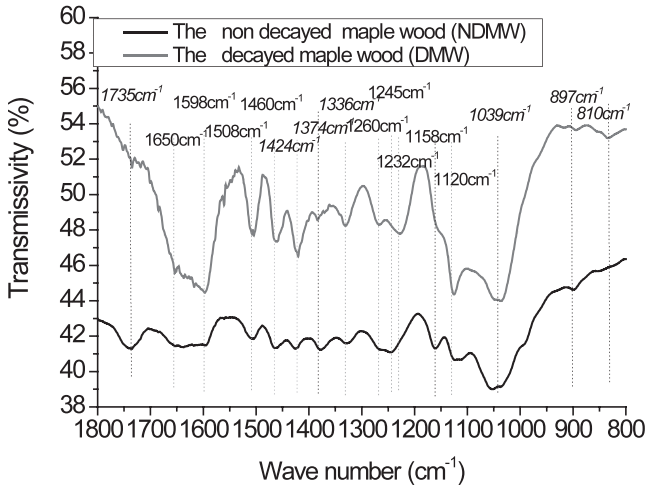

Figure 4.—Infrared spectrum of the maple wooden component: region from 1,800 to 800 cm^{-1}.

Table 2 shows that the content of lignin in DMW increased by about eightfold in I1508/I1735 and 14-fold in I1508/I1374, respectively, whereas those of cellulose and hemicellulose decreased evidently in I1735/I1508, I1374/I1508, I1159/I1508, and I897/I1508. The results further indicated that cellulose and hemicellulose in DMW were seriously degraded and harmed not only by insects but also by brown-rot fungi. The results are consistent with the visual spectrogram (Fig. 4). The index value of the cellulose crystallinity of I1374/I2900 decreased by 85.29 percent and that of I1424/I897 decreased by 47.67 percent (Table 2), indicating that the crystalline zones of cellulose were greatly degraded by brown-rot fungi.

Discussion

The wooden components, especially the eaves pillars, in ancient Danxia Temple buildings have been exposed to the air for a long time, so they were affected by multiple factors such as environmental temperature and humidity changes, microorganisms, insects, ultraviolet rays, and so on. Studies in the paper have shown that lignin has an adhesive role and is retained at higher levels; those of cellulose, which has a framework role, and hemicellulose, which has an interstitial filling role, were consumed seriously by brown-rot fungi, whether red oak, birch, or maple wooden components.

In addition to the decay caused by brown-rot fungi in the birch and maple wooden components, they were also attacked by insects, the damage being visible to the naked eye. Some studies (Graham 1967, Guo et al. 2010) have shown that fungi can attack woods and make them soft, decaying them and making it easier for insects to gnaw; for example, the dampwood termite can attack decayed woods but not nondecayed woods. The combination of fungi and insects accelerated the destruction of DBW and DMW. Even if the insects do not attack the decayed woods, these insects hollowed out the decayed woods, built nests, and lived in nests, eventually destroying the wooden components of the ancient buildings. Further study (Guo et al. 2010) has shown that the decayed woods can emit products that have a smell similar to that of pheromones, such as vanillic acid, hydroxybenzoic acid, coumaric acid, and so on, that attract insects. For example, termites and ants can use pheromones to mark their feeding paths, thus invading woods. The degradation of wooden components in the ancient buildings of Danxia Tample will eventually lead to a decrease in their strength and bearing capacity.

Conclusions

The absorption peak intensities, the changes in chemical components, and cellulose crystallinity of red oak, birch, and maple wooden components in the ancient buildings of Danxia Tample were analyzed with FTIR spectra. For the red oak, birch, or maple wooden components, part of absorption peak intensities that represent cellulose and hemicellulose decreased and disappeared obviously, whereas those representing lignin increased. The indexes of the contents of cellulose and hemicellulose and the cellulose crystallinity also decreased, whereas those of lignin increased. Those results indicated that cellulose and hemicellulose in the three woods were largely degraded by brown-rot fungi. In additional, both DBW and DMW were seriously harmed by insects, in addition to the attack of brown-rot fungi. The research of decay extent in this paper

can supply scientific data for later protection and repairs in Danxia Tample.

Acknowledgments

The authors gratefully acknowledge financial support from the Cross-Science Research Project of Nanyang Institute of Technology (230068), and Scientific Research Start-up Projects of Nanyang Institute of Technology (510144).

Literature Cited

Arias, M. E., J. Rodríguez, M. I. Pérez, M. Hernández, O. Polvillo, J. A. González-Pérez, and F. J. González-Vila. 2010. Analysis of chemical changes in *Picea abies* wood decayed by different *Streptomyces* strains showing evidence for biopulping procedures. *Wood Sci. Technol*. 44(2):179–188. DOI:10.1007/s00226-009-0282-1

Bari, E., G. Daniel, N. Yilgor, J. S. Kim, M. A. Tajick-Ghanbary, A. P. Singh, and J. Ribera. 2020. Comparison of the decay behavior of two white-rot fungi in relation to wood type and exposure conditions. *Microorganisms* 8. DOI:10.3390/microorganisms8121931

Bari, E., M. G. Daryaei, M. Karim, M. Bahmani, O. Schmidt, S. Woodward, M. A. T. Ghanbary, and A. Sistani. 2019. Decay of *Carpinus betulus* wood by *Trametes versicolor*—an anatomical and chemical study. *Int. Biodeterior*. *Biodegradation* 137:68–77. DOI:10.1016/j.ibiod. 2018.11.011

Bhatt, I. M., S. Pramod, R. D. Koyani, and K. S. Rajput. 2016. Anatomical characterization of *Eucalyptus globulus* wood decay by two white rot species of *Trametes*. *J. Plant Pathol*. 98(2):227–234. DOI:10.4454/JPP.V98I2.031

Brischke, C., S. Stricker, L. Meyer-Veltrup, and L. Emmerich. 2019. Changes in sorption and electrical properties of wood caused by fungal decay. *Holzforschung* 73(5):445–455. DOI:10.1515/hf-2018-0171

Chang, L., B. M. Rong, G. Xu, Q. Meng, and L. Wang. 2019. Mechanical properties, components and decay resistance of *Populus davidiana* bioincised by *Coriolus versicolor*. *J. Forestry Res*. 31:2023–2029. DOI:10.1007/s11676-019-00972-3.

Choi, J. W., D. H. Choi, S. H. Ahn, S. S. Lee, M. K. Kim, D. Meier, O. Faix, and G. M. Scott. 2006. Characterization of trembling aspen wood (*Populus tremuloides* L.) degraded with the white rot fungus *Ceriporiopsis subvermispora* and MWLs isolated thereof. *Holz als Roh Werkstoff* 64(5):415–422. DOI:10.1007/s00107-006-0133-9

Croitoru, C., C. Spirchez, A. Lunguleasa, D. Cristea, I. C. Roata, M. A. Pop, T. Bedo, E. M. Stanciu, and A. Pascu. 2018. Surface properties of thermally treated composite wood panels. *Appl. Surf. Sci*. 438:114–126. DOI:10.1016/j.apsusc.2017.08.193

Diandari, A. F., Djarwanto, L. M. Dewey, and Iriawati. 2020. Anatomical characterization of wood decay patterns in *Hevea brasiliensis* and *Pinus merkusii* caused by white-rot fungi: *Polyporus arcularius* and *Pycnoporus sanguineus*. *IOP Conf. Ser.: Earth Environ. Sci.* 528. DOI:10.1088/1755-1315/528/1/012048

Dong, S. H., C. Wang, J. K. Xiang, and G. Zhang. 2020. Research on changes of chemical composition and structure of the minor carpentry work in Gongshu Hall of Hu County based on FTIR—ATR. *Infrared* 41(7):30–37. DOI:10.3969/j.issn.1672-8785.2020.07.006

Fahey, L. M., M. K. Nieuwoudt, and P. J. Harris. 2019. Predicting the cell-wall compositions of solid *Pinus radiata* (radiata pine) wood using NIR and ATR FTIR spectroscopies. *Cellulose* 26(13–14): 7695–7716. DOI:10.1007/s10570-019-02659-8

Ferraz, A., and N. Durán. 1995. Lignin degradation during softwood decaying by the ascomycete *Chrysonilia sitophila*. *Biodegradation* 6(4):265–274. DOI:10.1007/BF00695257

Gao, S., X. Q. Yue, and L. H. Wang. 2019. Effect of the degree of decay on the electrical resistance of wood degraded by brown-rot fungi. *Can. J. Forest Res*. 49(2):145–153. DOI:10.1139/cjfr-2018-0282

Girometta, C., D. Dondi, R. M. Baiguera, F. Bracco, D. S. Branciforti, S. Buratti, S. Lazzaroni, and E. Savino. 2020. Characterization of mycelia from wood-decay species by TGA and IR spectroscopy. *Cellulose* 27:6133–6148. DOI:10.1007/s10570-020-03208-4

Graham, K. 1967. Fungi–insect mutualism in trees and timber. *Ann. Rev. Entomol*. 12:105–122.

Guo, M. L., H. F. Lan, and J. Qiu. 2010. Wood Deterioration and Preservation. China Metrology Publishing House, Beijing.

Ibrahim, M. N. M., N. N. M. Yusof, and A. Hashim. 2007. Comparison studies on soda lignin and soda anthraquinone lignin. *Malays*. *J. Anal. Sci*. 11(1):206–212.

Koyani, R. D., and K. S. Rajput. 2014. Light microscopic analysis of *Tectona grandis* L.f. wood inoculated with *Irpex lacteus* and *Phanerochaete chrysosporium*. *Eur. J. Wood Wood Prod*. 72(2):157–164. DOI:10.1007/s00107-013-0763-7

Li, G. Y., A. M. Huang, T. F. Qin, and L. H. Huang. 2010. FTIR studies of Masson pine wood decayed by brown-rot fungi. *Spectrosc. Spec. Anal*. 30(8):2133–2136. DOI:10.3964/j.issn.1000-0593(2010)08-2133-04

Li, S., Y. Gao, M. Brunetti, N. Macchioni, M, Nocetti, and S. Palanti. 2019. Mechanical and physical properties of *Cunninghamia lanceolata* wood decayed by brown rot. *iForest* 12:317–322. DOI:10.3832/ifor2922-012

Liu, C. W., M. L. Su, X. W. Zhou, R. J. Zhao, J. X. Lu, and Y. R. Wang. 2017. Analysis of content and distribution of lignin in cell wall of transgenic poplar with Fourier infrared spectrum (FTIR) and confocal laser scanning microscopy (CLSM). *Spectrosc. Spec. Anal*. 37(11):3404–3408. DOI:10.3964/j.issn.1000-0593(2017)11-3404-05

Monrroy, M., I. Ortega, and M. Ramirez. 2011. Structural change in wood by brown rot fungi and effect on enzymatic hydrolysis. *Enzyme Microb. Technol*. 49(5):472–477. DOI:10.1016/j.enzmictec. 2011.08.004

Murace, M. A., M. L. Luna, G. D. Keil, and N. N. De Cristófano. 2006.Anatomical changes in willow wood decayed by the brown rot fungus *Coriolellus malicola* (Basidiomycota). *Bol. Soc. Argent. Bot*. 41(3-4):159–166.

Padhiar, A., and S. Albert. 2011. Anatomical changes in *Syzygium cumuini* Linn. wood decayed by two white rot fungi *Schizophyllum commune* Fries. and *Flavodon flavus* (Klotzsch) Ryvarden. *J. Ind. Acad. Wood Sci*. 8(1):11–20. DOI:10.1007/s13196-011-0017-4

Padhiar, A., and S. Albert. 2012. Anatomical studies on decaying wood of Mangifera indica by two white rot fungi *Schizophyllum commune* and *Flavadon flavus*. *J. Ind. Acad. Wood Sci*. 9(2):143–153. DOI:10.1007/s13196-012-0079-y

Pandey, K. K. and H. C. Nagveni. 2009. Rapid characterisation of brown and white rot degraded chir pine and rubberwood by FTIR spectroscopy. *Holz als Roh Werkstoff* 65(6):477–481. DOI:10.1007/s00107-007-0181-9

Pandey, K. K., and A. J. Pitman. 2003. FTIR studies of the changes in wood chemistry following decay by brown-rot and white-rot fungi. Int. Biodeterior. *Biodegradation* 52(3):151–160. DOI:10.1016/S0964-8305(03)00052-0

Sanghvi, G. V., R. D. Koyani, and K. S. Rajp. 2013. Anatomical characterisation of teak (*Tectona grandis*) wood decayed by fungus *Chrysosporium asperatum*. *J. Trop. Forest Sci*. 25(4):547–553. DOI:10.2307/23616996

Stark, N. M., and L. M. Matuana. 2004. Surface chemistry changes of weathered HDPE/wood-flour composites studied by XPS and FTIR spectroscopy. *Polym. Degrad*. *Stab*. 86(1):1–9. DOI:10.1016/j.polymdegradstab. 2003.11.002

Stark, N. M., and L. M. Matuana. 2007. Characterization of weathered wood–plastic composite surfaces using FTIR spectroscopy, contact angle, and XPS. *Polym. Degrad*. *Stab*. 92(10):1883–1890. DOI:10.1016/j.polymdegradstab.2007.06.017

Sun, H., Y. Yang, Y. X. Han, M. J. Tian, B. Li, L. Han, A. F. Wang, W. Wang, R. Zhao, and Y. M. He. 2020. X-ray photoelectron spectroscopy analysis of wood degradation in old architecture. *BioResources* 15(3):6332–6343. DOI:10.15376/biores.15.3.6332-6343

Tamburini, D., J. J. Lucejko, B. Pizzo, M. Y. Mohammed, and R. Sloggett. 2017. A critical evaluation of the degradation state of dry archaeological wood from Egypt by SEM, ATR-FTIR, wet chemical analysis and Py(HMDS)-GC-MS. *Polym. Degrad. Stab*. 146:140–154. DOI:10.1016/j.polymdegradstab.2017.10.009

Tomak, E. D., E. Topaloglu, E. Gumuskaya, U. C. Yildiz, and N. Ay. 2013. An FT-IR study of the changes in chemical composition of bamboo degraded by brown-rot fungi. *Int. Biodeterior*. *Biodegradation* 85:131–138. DOI:10.1016/j.ibiod.2013.05.029

Wentzel, M., A. Rolleri, H. Pesenti, and H. Militz. 2019. Chemical

analysis and cellulose crystallinity of thermally modified *Eucalyptus nitens* wood from open and closed reactor systems using FTIR and X-ray crystallography. *Eur. J. Wood Wood Prod*. 77(4):517–525. DOI:10.1007/s00107-019-01411-0

Win, E., S. Takemoto, W. J. Hwang, M. Takeuchi, T. Itoh, and Y. Imamura. 2008. Anatomical characterization of decayed wood in standing light red meranti and identification of the fungi isolated from the decayed area. *J. Wood Sci*. 54(3):233–241. DOI:10.1007/s10086-008-0947-7

Xu, G. Q., L. H. Wang, J. L. Liu, and J. Z. Wu. 2013. FTIR and XPS analysis of the changes in bamboo chemical structure decayed by white-rot and brown-rot fungi. *Appl. Surf. Sci*. 280:799–805. DOI:10.1016/j.apsusc.2013.05.065

Yang, Y., J. X. Lu, and B. Li. 2020c. The mathematical model of heat and mass transfer in Alder birch wood and the color control during the thermo-vacuum treatment. *Chemical Industry Press*, Beijing. 108 pp.

Yang, Y., H. Sun, B. Li, L. Han, A. F. Wang, W. Wang, Y. M. He, and R. Zhao. 2020a. Study on the identification and the extent of decay of the wooden components in the Xichuan Guild Hall ancient architectures. *Int. J. Archit. Herit*. DOI:10.1080/15583058.2020.1786190

Yang, Y., H. Sun, B. Li, A. F. Wang, R. Zhao, W. Wang, Y. M. He, S. Yang, Y. X. Han, and W. Y. Sun. FTIR analysis of the chemical composition changes of wooden components in the ancient architectures of Xichuan Guild Hall. *Forest Prod. J.* 2020b. DOI:10.13073/FPJ-D-20-00028

Yang, Y., T. Y. Zhan, J. X. Lu, and J. H. Jiang. 2015. Influences of thermo-vacuum treatment on colors and chemical compositions of alder birch wood. *BioResources* 10(4):7936–7945. DOI:10.15376/biores.10.4.7936-7945

Zeng, Y. L., X. W. Yang, H. B. Yu, X. Y. Zhang, and F. Ma. 2012. The delignification effects of white-rot fungal pretreatment on thermal characteristics of moso bamboo. *Bioresour. Technol*. 114:437–442. DOI:10.1016/j.biortech.2011.10.036